

Magnetic phase diagram of RbMnBr_3 investigated by specific heat and magnetocaloric effect

F. Pérez, T. Werner, J. Wosnitza, and H. v. Löhneysen
Physikalisches Institut, Universität Karlsruhe, D-76128 Karlsruhe, Germany

H. Tanaka
Department of Physics, Faculty of Science, Tokyo Institute of Technology, Tokyo 152, Japan
 (Received 23 February 1998)

We report on high-resolution measurements of the specific heat and magnetocaloric effect of the distorted triangular lattice antiferromagnet RbMnBr_3 . Zero-field specific-heat data show a clear anomaly at $T_{c1} = 8.54$ K and a second shoulderlike anomaly about 35 mK above the first one. We study the evolution of these anomalies in applied external fields along the c axis and in the basal plane. We present a detailed magnetic phase diagram for $B \perp c$ for fields up to 7 T which is compared with earlier neutron scattering results and theoretical work. [S0163-1829(98)06938-0]

I. INTRODUCTION

Many ABX_3 compounds, where A^+ stands for an alkaline-metal ion, B^{2+} for a transition-metal ion, and X^- for a halogenide ion, crystallize in a hexagonal structure with the space-group $P6_3/mmc$. The relevant magnetic B^{2+} ions form triangular two-dimensional lattices within the ab plane, which are stacked along the c axis. The dominant magnetic interaction is via superexchange involving the nonmagnetic X^- ions. The superexchange is much stronger in c direction than in the plane. Therefore, these materials behave magnetically as quasi-one-dimensional systems at high temperatures, and often undergo a phase transition to a three-dimensionally (3D) ordered state at a low critical temperature T_c (typically around 10 K) where the weak magnetic coupling in the ab plane becomes important. In case of an antiferromagnetic ab exchange the spins are highly frustrated in the ordered state due to their triangular arrangement. Spin frustration leads to interesting magnetic (B, T) phase diagrams with unusual spin configurations¹ and to an unusual critical behavior.²

An example for an ideal triangular antiferromagnet is the well-studied compound CsMnBr_3 . This material keeps the undistorted hexagonal structure down to lowest temperatures. Because of an additional easy-plane anisotropy the spins are confined in the ab plane (XY system). Below the Néel temperature $T_N = 8.37$ K the nearest-neighbor spin vectors form angles of 120° to each other.³ This 120° spin structure is associated with the wave vector $\vec{Q} = (1/3, 1/3, 1)$ which is commensurate with the underlying lattice. A discrete additional symmetry, chirality, is broken in the ground state of this and related systems. Loosely speaking, the chirality reflects the handedness of the 120° spin structure around a triangular plaquette. For a chiral XY system critical exponents are predicted that significantly differ from the well established values for conventional 3D systems.² The largest deviation is found in the critical exponent α for the specific heat. An exponent $\alpha = 0.40 \pm 0.05$ was obtained for CsMnBr_3 ^{4,5} in good agreement with the predicted XY -chiral exponent² $\alpha = 0.34 \pm 0.06$. In fields applied along a direction within the ab plane the single transition of

CsMnBr_3 at zero field splits and a spin-flop (SF) phase arises between the 120° phase and the disordered paramagnetic (PM) phase. In the SF phase the spins are aligned collinearly perpendicular to the applied field in the ab plane, two thirds of them pointing in the same direction. The transition point at zero field is a tetracritical point.³

The closely related compound RbMnBr_3 undergoes several crystallographic phase transitions from the ideal hexagonal structure to a less symmetric low-temperature structure, which has up to date not been clearly determined.⁶ The possible orthorhombic crystal distortion leads to nonequivalent bond lengths in the ab plane, thus increasing the nearest-neighbor exchange along one of the three 120° directions which results in a partial release of frustration. Partially frustrated systems like RbMnBr_3 show novel physical phenomena that are absent in the fully frustrated systems. Glinka *et al.*⁷ found by neutron diffraction measurements that below $T_N = (8.8 \pm 0.1)$ K the spins form a spiral that differs from the simple triangular arrangement found in CsMnBr_3 in that the turn angle is about 130° instead of 120° . The corresponding wave vectors, for example, $\vec{Q} = (1/3 + \theta/2\pi, 1/3 + \theta/2\pi, 1)$, in this case are incommensurate with respect to the underlying lattice. The spin arrangement has been theoretically explained by assuming two magnetic interactions $J_{\perp 1}$ and $J_{\perp 2}$ in the basal plane differing in strength.^{8,10} According to Kawamura the incommensurability resulting from a lattice distortion is an irrelevant perturbation at the chiral critical point and the critical behavior should be the same as in the undistorted system CsMnBr_3 .⁸ On the other hand, the existence of a true chiral transition fixed point is questioned by some theoretical work⁹ which instead suggest a crossover to a first-order transition very near at T_N .

Another motivation for this work comes from the complex magnetic phase diagram of RbMnBr_3 . For fields applied within the ab plane new magnetic phases have been observed corresponding to spin arrangements that are not seen in the fully frustrated system. Almost simultaneously Kato *et al.*¹¹ and Heller *et al.*¹² presented (B, T) phase diagrams based on neutron diffraction studies which showed besides an assumed tetracritical point at zero field another

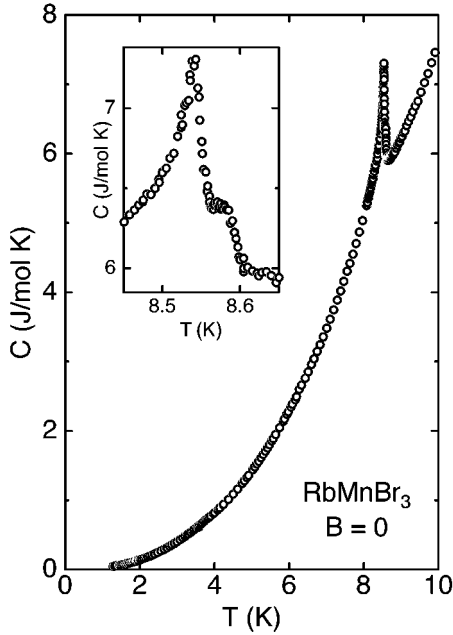


FIG. 1. Specific heat C vs temperature T of RbMnBr₃ in zero magnetic field. The inset shows the data near $T_N = 8.54$ K, revealing a shoulderlike anomaly about 35 mK above T_N .

multicritical point at¹² $T_{mc} = (7.8 \pm 0.1)$ K and $B_{mc} = (2.55 \pm 0.05)$ T. Both studies disagree about the number of phase lines merging at the latter critical point. The (B, T) phase diagram of RbMnBr₃ was investigated theoretically within a Ginzburg-Landau approach assuming an orthorhombic distortion of the ideal hexagonal lattice. The present study is aimed at exploring the phase diagram in detail. Our measurements reveal a splitting of the zero-field transition, thus the tetracritical point is “removed.”

II. EXPERIMENT

The investigated RbMnBr₃ single crystal was grown from powder by the Bridgman technique. The specific heat C was measured between 1.5 K and 30 K by a standard semiadiabatic heat-pulse technique in a ⁴He cryostat. The temperature resolution of $\delta T/T < 5 \times 10^{-6}$ allows small heat pulses with temperature increments $\Delta T/T = 100(\delta T/T) < 5 \times 10^{-4}$ at the transitions (< 5 mK for the RbMnBr₃ transitions). The absolute value of the measured temperatures may be wrong by $\pm 1\%$ due to a calibration error of the thermometer. The sample masses of about 40 mg yield a considerable sample contribution to the total heat capacity ($\geq 75\%$ in the whole relevant temperature range) and allow the determination of C with an absolute accuracy of $\approx 3\%$, the experimental resolution of C being better than 0.5%. The crystal orientation with respect to the magnetic-field direction is done visually using the freshly cleaved planes of the samples. The sample dimensions are approximately $10 \times 4 \times 2$ mm³. The largest dimension is parallel to the crystallographic c direction.

The measurements of the magnetocaloric effect $(\delta T/\delta B)_S = -(T/C)(\delta S/\delta B)_T$ were done in the same calorimeter. By changing the magnetic field in steps of $\Delta B \approx 30$ mT a variation of ΔT in the sample temperature is

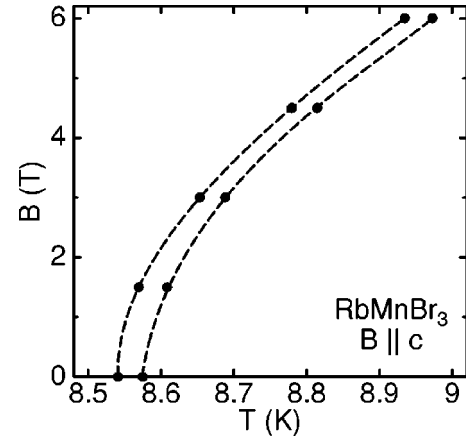


FIG. 2. Magnetic phase diagram of RbMnBr₃ for $B \parallel c$. The dashed lines are guides to the eye.

achieved. The sweep time for the change ΔB is kept long enough to keep eddy-current heating low and short enough to measure ΔT in the same adiabatic fashion as for the specific heat. Eddy-current heating is determined by sweeping ΔB up and down and averaging the ensuing temperature changes. The magnetocaloric effect results as $\Delta T/\Delta B$. The demagnetization effect of RbMnBr₃ is negligible in our experiment, as estimated from its small magnetization.²⁰

The combination of specific-heat and magnetocaloric-effect measurements allows us to map out the (B, T) plane in T (specific heat) and B (magnetocaloric effect) direction.

III. RESULTS AND DISCUSSION

Figure 1 shows the specific heat of RbMnBr₃ at $B=0$ in the temperature range between 1.5 and 9.5 K. A clear anomaly at $T_{c1} = T_N = (8.540 \pm 0.006)$ K can be seen. Compared to our earlier CsMnBr₃ specific-heat data⁵ at zero field, the divergence in RbMnBr₃ is much weaker. The expansion of the T axis around the anomaly shown in the inset of Fig. 1 reveals a second shoulderlike anomaly at T_{c2} , about 35 mK above T_{c1} . To our knowledge the existence of the shoulderlike anomaly at T_{c2} has not been reported previously. Measurements on a second sample proved the reproducibility of the obtained results. Therefore impurities or different phases in the samples are unlikely to cause the double feature.

Apparently the intermediate magnetic phase SF₁, occurring between the incommensurate triangular spin structure with chiral symmetry (C_1) and the paramagnetic (PM) one, is stabilized even at zero field. Because of its extreme narrowness an unambiguous extraction of the critical exponent α is not possible. The value for the critical exponent $\beta = 0.28 \pm 0.02$ given in Ref. 13, although determined using only data for temperatures $T < T_N$, seems to be questionable in the light of this new experimental finding. Furthermore, our experimental data are incompatible with the existence of a tetracritical point at $B=0$, like the one seen in the phase diagram of the fully frustrated system CsMnBr₃.³⁻⁵ This fact might also explain the weaker divergence of RbMnBr₃ compared with the one of CsMnBr₃ at zero field. For RbMnBr₃ the lattice distortion (probably orthorhombic) leads to $J_{\perp 1} \neq J_{\perp 2}$ and hence to an incommensurate spin structure at zero field.⁸ For a lattice distortion keeping the hexagonal symme-

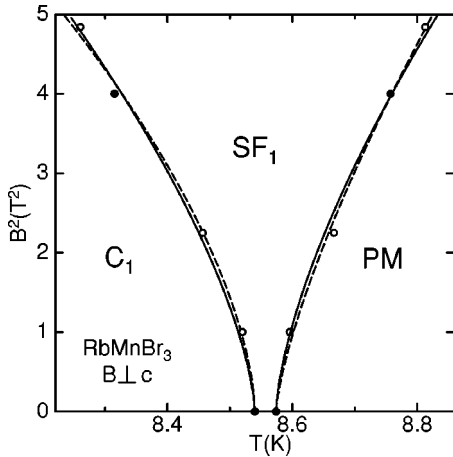


FIG. 3. Magnetic phase diagram of RbMnBr_3 for $B \perp c$ with $B \leq 2.25$ T plotted as B^2 vs T . The lines correspond to fits using Eq. (1) with $\phi_1=0.61$, $\phi_2=0.73$ (dashed lines), and $\phi_1=\phi_2=0.66$ (solid lines).

try, applicable to RbFeBr_3 or RbVBr_3 ,¹⁵ Plumer *et al.*¹⁴ predict an intermediate linearly polarized phase. In this case the inequivalence $J_{\perp 1} \neq J_{\perp 2}$ acts as an effective field in the ab plane of the XY system. To our knowledge, corresponding calculations do not exist for the presumably orthorhombic symmetry of RbMnBr_3 . Therefore, the existence of an intermediate phase in zero field should serve as an input to treat the case of a general distortion of the hexagonal ab planes theoretically.

With increasing field applied along the c direction of the sample both transition temperatures T_{c1} and T_{c2} increase slightly, remaining equidistant up to $B=6$ T. The resulting (B, T) phase diagram is shown in Fig. 2. Below T_{c1} the magnetic structure is probably an incommensurate umbrella-like structure, the planar spins canting gradually out of the plane into the field direction. The phase boundary bends towards higher temperatures with increasing field.

For fields parallel to the basal plane ($B \perp c$) a drastic change in the phase-diagram topology is observed (see Fig. 3). The two transition points at $B=0$ split with increasing field and the SF_1 phase quickly widens. The zero-field anomaly at T_{c1} weakens while the one at T_{c2} sharpens until at 2 T they are of the same magnitude (see Fig. 4).

In the limit $B \rightarrow 0$, the two transition boundaries emanating from the tetracritical point of the ideal XY system are predicted to behave as

$$B^2 = w_i |T_{ci}(B) - T_c(0)|^{\phi_i}, \quad (1)$$

where $i=1$ and $i=2$ stand for the chiral-spinflop and spinflop-paramagnetic boundaries, respectively. Renormalization group calculations¹⁶ predict that the crossover exponents ϕ_1 and ϕ_2 should be equal ($\phi_1 = \phi_2 = \phi_{th} = 1.04$). ϕ_{th} and the ratio w_1/w_2 should be universal quantities. For CsMnBr_3 $\phi_1 = \phi_2 = 0.77 \pm 0.12$ and $w_1/w_2 = 1.05 \pm 0.2$ was estimated¹⁷ for $B \leq 2$ T. Although not dealing with an ideal XY system we attempt a similar fit on the low-field data $B \leq 2.25$ T of RbMnBr_3 (see Fig. 3). $T(0)$ in Eq. (1) is substituted by $T_{c1}(0)$ and $T_{c2}(0)$. The crossover exponents are found to be $\phi_1 = 0.61 \pm 0.1$ and $\phi_2 = 0.73 \pm 0.1$. A fit with the constraint of the theoretical prediction

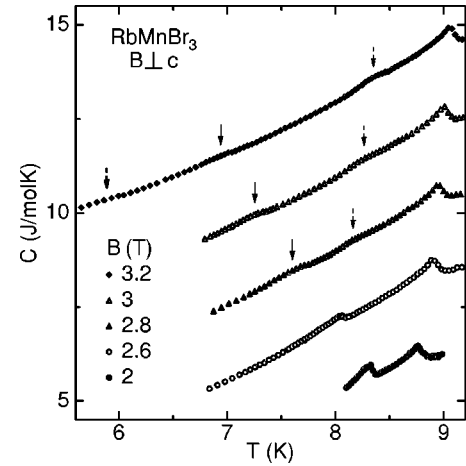


FIG. 4. Specific heat C vs temperature T of RbMnBr_3 for magnetic fields $2 \text{ T} \leq B \leq 3.2 \text{ T}$ ($B \perp c$). For clarity, the values of C are shifted upward consecutively by 2 J/mol K with increasing field. The arrows denote the estimated transition temperatures.

$\phi_1 = \phi_2 = \phi$ is also possible within the error bars and yields $\phi = 0.66 \pm 0.1$ and $w_1/w_2 = 1.1 \pm 0.2$. Although RbMnBr_3 exhibits a zero-field T_c splitting these values agree surprisingly well with those found for CsMnBr_3 with a tetracritical point at $B=0$. The experimental values for ϕ in both cases are at variance with theoretical predictions.

Figures 4 and 5 show our specific-heat data at intermediate and high magnetic fields. Up to $B=2.6$ T the T region of the intermediate phase SF_1 widens. An additional anomaly between T_{c1} and T_{c2} appears for $B=2.8$ T at $T_{c3} = (8.16 \pm 0.08)$ K. Here, the temperature interval between T_{c3} and the anomaly at T_{c2} remains roughly constant with increasing field up to 7 T. Both anomalies shift towards higher temperatures and become somewhat more pronounced with field. At $B=3.2$ T a fourth anomaly can be resolved below the one at T_{c1} .

In order to allow a better estimation of the critical temperatures of the weak anomalies around 3 T, we proceed as

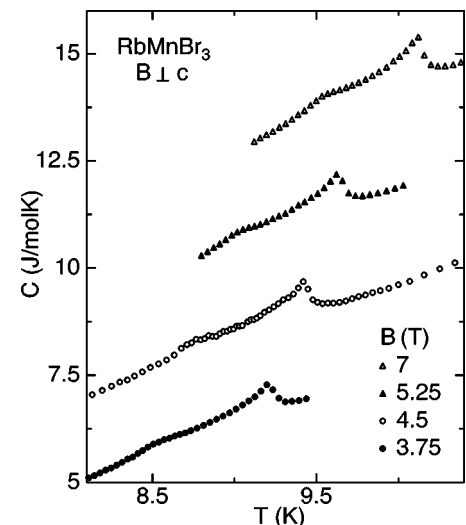


FIG. 5. Specific heat C vs temperature T of RbMnBr_3 for magnetic fields $B \geq 3.75$ T ($B \perp c$). For clarity, the values of C are shifted upward consecutively by 2 J/mol K with increasing field.

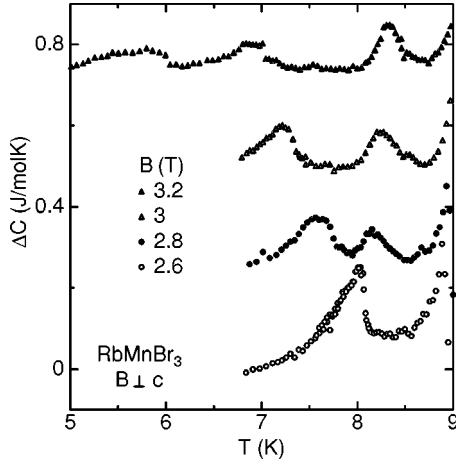


FIG. 6. ΔC vs temperature T of RbMnBr₃ for fields around 3 T. ΔC results from the difference of the measured specific heat and a second order polynomial fit C_{pol} to the 3.2 T data (see text).

follows. A polynomial of second order, C_{pol} , is fitted to those data points at $B=3.2$ T between 4.5 and 8.8 K that are far enough from the critical temperatures of the anomalies below T_{c2} . In this way we approximate the contributions to the specific heat that are not related to the singularities at and near 3.2 T. The difference ΔC between the measured specific heat and the fitted function C_{pol} is shown in Fig. 6.

Magnetocaloric-effect measurements at $T=3, 4.5, 5.5, 6.4,$ and 7 K serve to complement our magnetic phase diagram of RbMnBr₃ for $B \perp c$. The data collected at $T=3, 4.5$ and 6.4 K are shown in Fig. 7. For all temperatures the overall magnetocaloric effect $\Delta T/\Delta B$ increases with increasing field. One should observe that the rising background does not depend monotonically on T . Two reproducible anomalies are resolved on each curve. The anomaly at lower fields, i.e. the maximum, weakens with increasing temperature and is barely visible at 6.4 K while the steplike anomaly at higher fields becomes more pronounced.

Our phase diagram for $B \perp c$ contains five different phases, which we call C_1, C_2, SF_1, SF_2 and PM (see Fig. 8). The phase diagram is in good agreement with earlier neutron scattering results from Kato *et al.*¹¹ and confirms the existence of the phase boundary C_2 - SF_2 which was questioned in

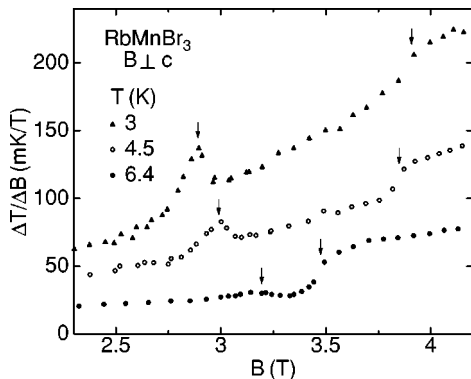


FIG. 7. Magnetocaloric effect $\Delta T/\Delta B$ vs magnetic field B of RbMnBr₃ for selected temperatures ($B \perp c$). The arrows denote the estimated transition fields. The $T=3$ K data have an offset of 60 mK/T.

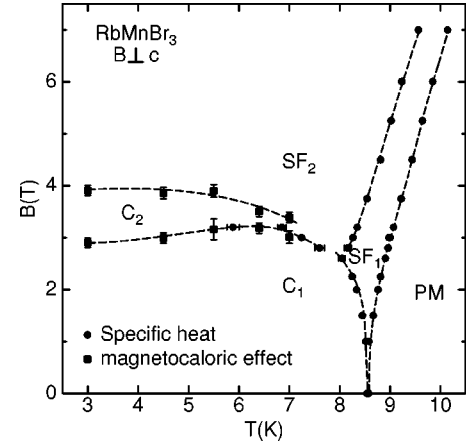


FIG. 8. Magnetic phase diagram of RbMnBr₃ for $B \perp c$. The points are extracted from our specific-heat and magnetocaloric-effect data. The dashed lines are guides to the eye.

Ref. 12. In the chiral phases C_1 and C_2 the order parameter is elliptically polarized. The polarization is linear in the spinflop-like phases SF_1 and SF_2 . Spin configurations C_1 and SF_1 are incommensurate with the same incommensurate ordering vector.¹² A simple thermodynamic consideration¹⁸, taking the sign of the specific heat and magnetocaloric effect “jumps” ($\Delta\alpha$ and $\Delta\beta$, respectively) at the transition line C_1 - C_2 into account, shows that the positive slope $(dB/dT)_{C_1-C_2} = \Delta\alpha_{C_1-C_2}/\Delta\beta_{C_1-C_2}$ of this boundary below its maximum, i.e., for $T \leq 6.5$ K, is incompatible with a second-order phase line. The transition C_1 - C_2 , therefore of first order, is characterized by a maximum in the magnetocaloric effect (see Fig. 7). On the other hand the steplike anomaly in the magnetocaloric effect at higher fields corresponds to a second-order transition.^{11,12,19} Our specific-heat data (Fig. 5) seem to point to second-order behavior for the remaining phase lines SF_2 - SF_1 and SF_1 -PM, although for the SF_2 - SF_1 transition first-order behavior has been suggested.¹²

Zhitomirsky¹⁹ explains qualitatively the diverse phase diagram of RbMnBr₃ for $B \perp c$ in a Landau approach using the “row” model. His analysis suggests that the four magnetically ordered phases should coexist at a multicritical point, which we estimate by extrapolating the phase boundaries C_1 - C_2 and SF_1 - SF_2 to $T_{\text{mc}} = (8.0 \pm 0.1)$ K and $B_{\text{mc}} = (2.6 \pm 0.2)$ T in good agreement with previous experimental determinations.¹² There is, however, a marked difference of the shape of the C_2 - SF_2 phase boundary between Ginzburg-Landau predictions and experiment.

IV. SUMMARY

We have observed an intermediate phase SF_1 in the phase diagram of RbMnBr₃ in a finite temperature region even at $B=0$. This intermediate phase has not been detected before, due to the extremely small stability range of ≈ 35 mK, which requires the high resolution in T achieved in our experiment. In fields applied parallel to the sample c axis the phase SF_1 remains narrow up to 6 T and shifts towards higher temperatures. In perpendicular fields a diverse phase diagram is found comprising a total of four magnetically ordered phases, which appear to coexist at the multicritical

point [$T_{mc}=(8.0\pm 0.1)$ K, $B_{mc}=(2.6\pm 0.2)$ T]. The latter phase diagram is in agreement with earlier experimental results^{11,20} and resembles the qualitative predictions of Zhitomirsky.¹⁹ An analysis of the $B\perp c$ case for fields $B\leq 2.25$ T leads to a crossover exponent $\phi=0.66\pm 0.1$ and

$w_1/w_2=1.1\pm 0.2$. It is surprising that these values are close to those for the ideal hexagonal-lattice system CsMnBr_3 which—in contrast to the distorted RbMnBr_3 —exhibits a tetracritical point at $B=0$. This point deserves further experimental and theoretical studies.

-
- ¹For a recent review on triangular antiferromagnets, see M. F. Collins and O. A. Petrenko, *Can. J. Phys.* **75**, 605 (1997).
- ²D. H. Lee, J. D. Joannopoulos, and J. W. Negele, *Phys. Rev. Lett.* **52**, 433 (1984); H. Kawamura, *J. Phys. Soc. Jpn.* **54**, 3220 (1985); **61**, 1299 (1992).
- ³B. D. Gaulin, T. E. Mason, M. F. Collins, and J. Z. Larese, *Phys. Rev. Lett.* **62**, 1380 (1989).
- ⁴J. Wang, D. P. Belanger, and B. D. Gaulin, *Phys. Rev. Lett.* **66**, 3195 (1991).
- ⁵R. Deutschmann, H. v. Löhneysen, J. Wosnitza, R. K. Kremer, and D. Visser, *Europhys. Lett.* **17**, 637 (1992).
- ⁶T. Kato, K. Iio, T. Hoshino, T. Mitsui, and H. Tanaka, *J. Phys. Soc. Jpn.* **61**, 275 (1992); T. Kato, K. Machida, T. Ishii, K. Iio, and T. Mitsui, *Phys. Rev. B* **50**, 13 039 (1994).
- ⁷C. J. Glinka, V. J. Minkiewicz, D. E. Cox, and C. P. Khattak, in *Magnetism and Magnetic Materials*, Proceedings of the 19th Annual Conference on Magnetism and Magnetic Materials, edited by C. D. Graham and J. J. Rhyne, AIP Conf. Proc. No. **18** (AIP, New York, 1973), p. 659.
- ⁸H. Kawamura, *Prog. Theor. Phys. Suppl.* **101**, 545 (1990).
- ⁹M. L. Plumer and A. Mailhot, *J. Phys.: Condens. Matter* **9**, L165 (1997).
- ¹⁰W. Zhang, W. M. Saslow, M. Gabay, and M. Benakli, *Phys. Rev. B* **48**, 10 204 (1993).
- ¹¹T. Kato, T. Ishii, Y. Ajiro, T. Asano, and S. Kawano, *J. Phys. Soc. Jpn.* **62**, 3384 (1993).
- ¹²L. Heller, M. F. Collins, Y. S. Yang, and B. Collier, *Phys. Rev. B* **49**, 1104 (1994).
- ¹³T. Kato, T. Asano, Y. Ajiro, S. Kawano, T. Ishii, and K. Iio, *Physica B* **213&214**, 182 (1995).
- ¹⁴M. L. Plumer, A. Caillé, and H. Kawamura, *Phys. Rev. B* **44**, 4461 (1991).
- ¹⁵H. Tanaka and K. Kakurai, *J. Phys. Soc. Jpn.* **63**, 3412 (1994).
- ¹⁶H. Kawamura, A. Caillé, and M. L. Plumer, *Phys. Rev. B* **41**, 4416 (1990).
- ¹⁷H. v. Löhneysen, D. Beckmann, J. Wosnitza, and D. Visser, *J. Magn. Magn. Mater.* **140-144**, 1469 (1995); H. Weber, D. Beckmann, J. Wosnitza, and H. v. Löhneysen, *Int. J. Mod. Phys. B* **9**, 1387 (1995).
- ¹⁸S. K. Yip, T. Li, and P. Kumar, *Phys. Rev. B* **43**, 2742 (1991); A. J. Leggett, *Prog. Theor. Phys.* **51**, 1275 (1974).
- ¹⁹M. E. Zhitomirsky, *Phys. Rev. B* **54**, 353 (1996).
- ²⁰Y. Ajiro, T. Asano, H. Kadowaki, T. Kato, S. Kawano, H. Aruga Katori, and T. Goto, *Physica B* **213&214**, 209 (1995).